Applied Science and Engineering Progress, Vol. 20, No. 1, 2027, 8253

Research Article

Morphological Transformation of Self-Assembled Platinum Nanodots on Isopropanol-Modified Quartz Substrate via Thermal Dewetting

Nopparat Seemuang
Department of Production and Robotics Engineering, Faculty of Engineering, King Mongkut's University of Technology North Bangkok, Bangkok, Thailand

Reungruthai Sirirak
School of Science, University of Phayao, Phayao, Thailand

Potejanasak Potejana*
Industrial Engineering Program, School of Engineering, University of Phayao, Phayao, Thailand

* Corresponding author. E-mail: potejanasak.po@up.ac.th DOI: 10.14416/j.asep.2026.07.007
Received: 16 February 2026; Revised: 17 March 2026; Accepted: 17 April 2026; Published online: 20 July 2026

Abstract

The controlled fabrication of platinum (Pt) nanodots on quartz substrates has attracted considerable attention for advanced applications in plasmonics, biosensing, catalysis, and nanoelectronic devices. In this study, the morphological transformation of thermally dewetted Pt thin films deposited on untreated and isopropanol (IPA)-modified quartz substrates was systematically investigated. Pt thin films with a thickness of approximately 10 nm were deposited using a sputter coating technique and subsequently annealed at temperatures ranging from 400 °C to 700 °C. The thermal dewetting behavior and morphological evolution of Pt nanostructures were systematically examined through hot stage-assisted in situ thermal annealing integrated with field-emission scanning electron microscopy (FE-SEM), combined with ImageJ-based quantitative surface coverage analysis. The results demonstrated that annealing temperature and substrate surface condition strongly influenced the dewetting behavior and final morphology of the Pt nanostructures. At lower annealing temperatures, the Pt films exhibited limited atomic diffusion and irregular fragmented structures, whereas higher temperatures promoted film breakup and the formation of isolated Pt nanodots. A significant difference in morphological evolution was observed between untreated and IPA-treated substrates. The untreated substrate retained partially interconnected Pt domains even at high annealing temperatures, indicating incomplete dewetting behavior. In contrast, the IPA-treated substrate facilitated the formation of smaller, more uniformly distributed, and well-separated Pt nanodots with reduced surface coverage, suggesting enhanced thermal dewetting and improved nanoparticle uniformity. In addition, absorbance spectra measurements revealed morphology-dependent optical responses associated with variations in Pt nanostructure size and particle distribution. The Pt nanodots formed on the IPA-treated substrate exhibited a higher, steeper absorbance peak than those formed on the untreated substrate, indicating improved nanoparticle uniformity and enhanced morphology-dependent optical interactions after thermal dewetting. The experimental results in this study clearly demonstrate the effect of IPA surface treatment on the morphological transformation and dewetting behavior of Pt thin films.

Keywords: Absorbance spectrum, Isopropanol-assisted substrate, Platinum nanodots, Nanostructure agglomeration, Thermal dewetting process

1 Introduction

Platinum (Pt) nanostructures are at the forefront of nanomaterials research due to their remarkable intrinsic properties, including high chemical stability, excellent electrical conductivity, superior catalytic activity, and strong interaction with electromagnetic radiation [1]-[5]. These properties make Pt

Applied Science and Engineering Progress, Vol. 20, No. 1, 2027, 8253

nanostructures indispensable in a wide range of high-performance applications, particularly in the fields of energy conversion, environmental sensing, and next-generation electronics [6]-[8]. Within the broader class of Pt nanostructures, Pt nanodots defined as discrete, zero-dimensional nanoparticles typically below 20 nm in diameter are of special interest. Their high surface-to-volume ratio dramatically enhances surface reactivity, enabling efficient catalytic performance in reactions such as the hydrogen evolution reaction (HER) and oxygen reduction reaction (ORR) [9]-[10]. Furthermore, their nanometric size introduces quantum confinement effects that modify their electronic density of states, enabling size-tunable functionalities in electronic and optical devices [11]-[12]. Pt nanodots also support localized surface plasmon resonance (LSPR) phenomena, despite being a transition metal, which allows them to be used in advanced plasmonic biosensors with enhanced sensitivity [13]-[14]. Moreover, their potential for controlled positioning on substrates opens pathways for integration into single-electron transistors and nanoelectronic circuitry [15]. The adaptability of Pt nanodots, particularly when formed on transparent and thermally stable substrates like glass, also makes them suitable for incorporation into flexible optoelectronic devices and photothermal therapy platforms, highlighting their cross-disciplinary relevance in both emerging technologies and fundamental science [16]-[18].

Thermal dewetting has emerged as a promising and scalable technique for fabricating metal nanodots on dielectric quartz substrates. Unlike lithographic or chemical approaches, thermal dewetting exploits the intrinsic thermodynamic instability of thin metal films under high-temperature conditions, causing the films to rupture and reorganize into discrete nanoparticles to minimize surface and interfacial energies. This process involves hole nucleation, growth, and the eventual breakup of the film into isolated nanodots, with the evolution strongly influenced by parameters such as film thickness, annealing temperature, and substrate surface energy [19]-[20]. Gold (Au) nanodots, known for their plasmonic properties, are typically formed via dewetting at 500–600 °C, with controlled size and spacing suitable for SERS and optical devices [21]-[24]. Silver (Ag), which dewets at lower temperatures (300–400 °C), offers strong localized surface plasmon resonance (LSPR) but requires precise conditions to prevent coarsening or oxidation [25]-[26]. Copper (Cu), despite its susceptibility to oxidation, can be used to produce nanodots at 400–500 °C when annealed in vacuum or reducing atmospheres, making it viable for photonic and sensor applications [27]. Platinum (Pt), with its high melting point and strong adhesion to oxide surfaces, generally requires higher annealing temperatures (≥600 °C) to induce dewetting, and pretreatment steps such as acetone cleaning or plasma exposure can enhance film instability and dot uniformity [28]-[29]. The resulting Pt nanodots exhibit remarkable thermal and chemical stability and are increasingly used in cutting-edge applications such as catalytic microreactors, electrochemical sensors, and nanophotonic energy devices. Overall, thermal dewetting offers a versatile and clean route to engineer metal nanostructures with tunable properties on glass substrates for various high-performance technologies [30]-[31].

The surface energy of quartz glass substrates critically influences the dewetting behavior and aggregation dynamics of metallic nanodots formed via thermal annealing. High-energy quartz surfaces, such as those treated by oxygen plasma or UV-ozone cleaning, enhance metal substrate adhesion and promote uniform nucleation of holes in thin films [32]-[33]. For gold (Au), increased surface energy facilitates early-stage rupture and yields well-ordered, size-controlled nanodots, whereas low-energy or contaminated surfaces delay dewetting and lead to irregular morphologies [34]. Silver (Ag), due to its high diffusivity and lower adhesion, dewets more rapidly on hydrophilic quartz surfaces, forming fine nanodots at relatively low temperatures; however, on low-energy surfaces, Ag tends to coarsen and aggregate [35]. Copper (Cu) shows improved dewetting behaviour when the quartz substrate is pretreated to enhance surface energy, forming fine nanodots under vacuum; otherwise, poor wettability and oxidation lead to inhomogeneous patterns [36]. Platinum (Pt), with its high melting point and strong adhesion, typically requires elevated temperatures to initiate dewetting, but substrate pretreatments such as plasma exposure significantly enhance film instability and promote uniform nanodot formation [37],[38]. Overall, tailoring the surface energy of quartz glass is essential for achieving controlled dewetting across different metals, affecting not only the onset temperature of film rupture but also the resulting nanodot size, spacing, and distribution.

In this study, the isopropanol (IPA) rinsing treatment was employed to modify the surface condition of the quartz glass substrate prior to platinum (Pt) film deposition. IPA is a polar solvent that effectively removes organic contaminants, surface hydrocarbons, and dust particles from the substrate surface. These contaminants typically reduce the surface energy and create nonuniformities that interfere with controlled film rupture during thermal dewetting. By eliminating these residues, IPA treatment exposes hydroxyl (–OH) groups on the quartz surface, making it more hydrophilic [39],[40]. This increase in surface energy improves the adhesion of the Pt thin film and enhances the wetting interaction between the metal and the substrate. As a result, the thermal dewetting process becomes more predictable and uniform. The cleaner substrate surface leads to a more uniform distribution of Pt nanodots and minimizes particle agglomeration after thermal dewetting. Consequently, the IPA-treated substrate promotes the formation of smaller and more uniformly distributed Pt nanodots. This improvement in nanodot quality is crucial for advanced applications in sensing, catalysis, and photonic devices, where performance is strongly dependent on nanoscale geometry and distribution.

2 Materials and Methods

2.1 *Self-organization of Pt nanodots by the thermal dewetting method.*

Using the thermal dewetting method for platinum (Pt) thin films provides a simple and high-throughput nanofabrication process for producing random nanostructures on solid substrates. In this process, a continuous Pt thin film initially deposited by sputtering is transformed into discrete nanoislands through solid-state dewetting driven by thermal energy [41]. When the Pt-coated substrate is heated to an appropriate annealing temperature, the system tends to minimize its total interfacial and surface energies. This energy minimization results in the agglomeration of Pt atoms and the morphological transition from a continuous film into isolated nanodots.

Figure 1 illustrates the agglomeration mechanism of the Pt thin film into nanodots on a substrate that proceeds in 4 stages. Firstly (i), thermal activation initiates the nucleation of nanoscale voids

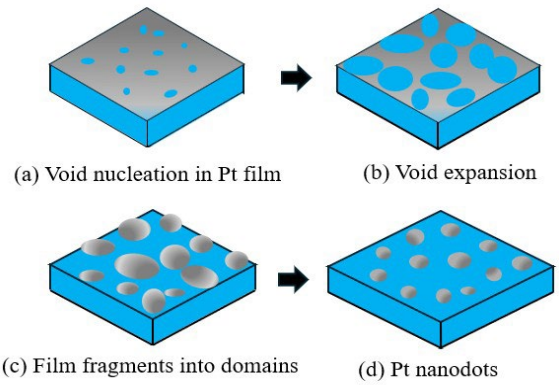

Figure 1: Schematic illustration of the morphological evolution and thermal dewetting process of Pt thin films on a quartz substrate leading to Pt nanodot formation.

at defects or grain boundaries within the Pt film. Secondly (ii), as annealing continues, these voids expand laterally due to enhanced atomic surface diffusion, causing the rupture of the continuous Pt layer. Then (iii), at optimal thermal dewetting temperature and duration, the void growth results in the fragmentation of the Pt film into isolated domains. Finally (iv), the atoms in these separated Pt regions move across the surface until each region shrinks and rounds off, turning into Pt nanodots on the substrate.

Key parameters influencing the final nanoparticle morphology include the initial Pt film thickness, substrate surface energy, annealing temperature, and annealing duration. Thinner Pt films tend to dewet and form smaller nanoparticles at lower temperatures, whereas thicker films require higher annealing temperatures to induce complete dewetting. While the thermal annealing approach offers the advantages of simplicity, low fabrication cost, and compatibility with large-area processing, it generally results in random nanoparticle size and spacing distributions. Nevertheless, Pt nanoislands fabricated by this method exhibit unique plasmonic, catalytic, and surface-enhanced optical properties, making them valuable for applications in sensing.

Figure 2 illustrates a schematic diagram of the experimental procedure for fabricating self-organized Pt nanodots on a quartz glass substrate via the thermal dewetting process. First (a), quartz glass sheets with a thickness of 1 mm were cut into 1 cm^2 pieces. The substrates were cleaned in an acetone bath using an

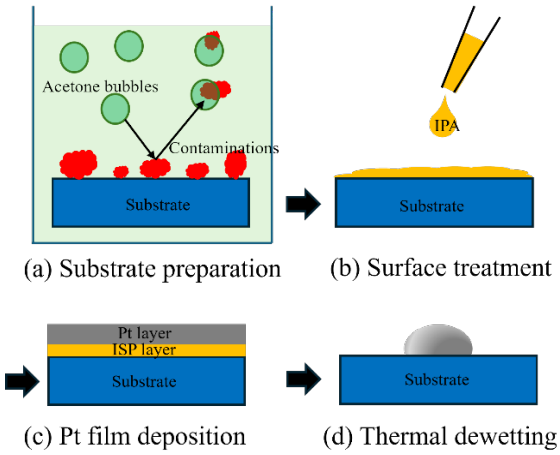

Figure 2: Schematic illustration of the experimental procedure for fabricating self-organized Pt nanodots on quartz substrates via thermal dewetting.

ultrasonic cleaner (GT Sonic, VGT-1613T) for 10 min to remove surface contaminants and residual impurities. Next (b), a drop of isopropanol was applied onto the cleaned substrate surface as a surface modification treatment prior to Pt deposition. Then (c), a thin platinum (Pt) film was deposited onto the IPA-treated substrate using a sputter coating system (DC-MCM-200 Ion Sputter Coater). Argon (Ar) gas was used as the sputtering gas at a pressure of 15 Pa. The acceleration voltage was set to 0.7 kV, while the sputtering current was maintained at 5 mA during the deposition process. The Pt target diameter was 50 mm, and the target-to-substrate distance was fixed at 35 mm. Prior to sputtering, the chamber was evacuated to a high vacuum of approximately 10^{-5} mbar. During sputtering, Pt atoms were ejected from the target and transported through the vacuum before being deposited onto the substrate surface. The Pt film thickness was controlled by adjusting the sputtering time, resulting in an approximate deposition rate of 5 nm/min. In this study, the Pt film thickness was fixed at approximately 10 nm. Finally (d), the Pt-coated substrates underwent self-organization through hot stage-assisted thermal dewetting of Pt films on quartz glass substrates.

2.2 *Hot stage-assisted thermal annealing of Pt films on quartz substrate*

The Gatan Murano hot stage was employed to enable real-time monitoring of the morphological transformation of platinum (Pt) nanodot arrays deposited on a quartz glass substrate. This advanced heating stage, designed for *in situ* experimentation, was integrated into a field-emission scanning electron microscope (FE-SEM, SU3500, Hitachi, Japan). By mounting the quartz substrate directly on the silicon-based heating element of the stage, it became possible to continuously observe the agglomeration and evolution of Pt nanostructures during simulated thermal treatments. The advantage of employing the Gatan Murano hot stage lies in its ability to replicate actual annealing processes in situ, while maintaining direct visualization of nanostructure evolution without the need to remove the sample from the microscope. This minimizes contamination risks, eliminates sample transfer errors, and allows researchers to precisely correlate morphological changes with applied thermal conditions.

The schematic representation of the setup is shown in Figure 3, where the quartz glass substrate coated with a thin Pt film was positioned on the heating stage. This configuration provided a highly stable environment for thermal dewetting while allowing the FE-SEM to capture surface changes in real time. The temperature range accessible by the stage extended from 400 to 700 °C, enabling systematic studies of nanoscale morphological evolution under controlled heating conditions.

In this study, the experimental design was systematically divided into two distinct batches in order to investigate the influence of substrate surface treatment on the agglomeration behavior of platinum thin films. For Batch 1, a platinum film with a nominal thickness of 10 nm was deposited directly onto the quartz glass substrate without any surface modification. This condition served as a reference for the natural dewetting and agglomeration behavior of Pt on a pristine substrate surface. In contrast, Batch 2 involved the deposition of a 10 nm Pt film onto a quartz glass substrate that had been pretreated with isopropanol (IPA). The surface modification by IPA was intended to alter the surface energy of the substrate and, consequently, influence the nucleation, diffusion, and breakup mechanisms of the Pt thin film during subsequent thermal dewetting treatment. By conducting a comparative investigation between Batch 1 and Batch 2, the study aimed to elucidate the extent to which surface pretreatment modifies the dynamics of agglomeration, the morphology of the resulting nanodots, and the overall stability of the self-

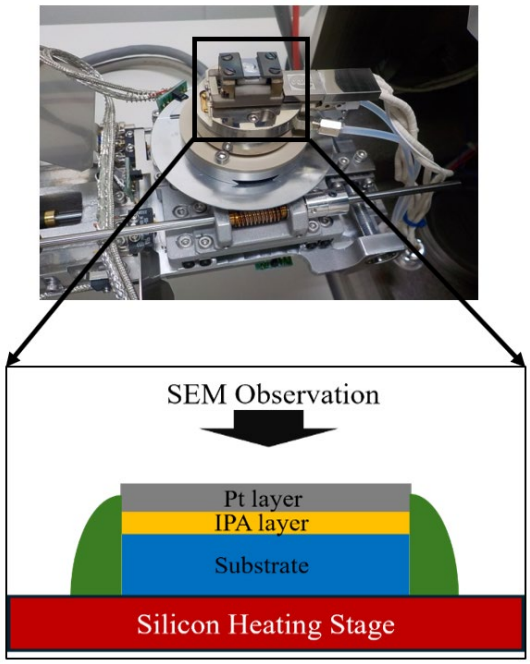

Figure 3 : Experimental setup for *in situ* hot stage-assisted thermal annealing of Pt thin films integrated with a field-emission scanning electron microscope (FE-SEM).

organized Pt nanostructures. Such a two-batch approach provides valuable insight into how subtle changes in the initial surface conditions can govern the evolution of thin metal films under thermal dewetting. Thermal annealing was performed from 400 to 700 °C, and the changes in the Pt film morphology were monitored stepwise at every 100 °C increment. These selected temperatures correspond to regimes where the thin Pt film underwent a transition from a continuous layer into isolated nanoislands through the process of solid-state dewetting.

3 Results and Discussion

3.1 *The agglomeration evolution of Pt film on the substrate*

The *in situ* thermal annealing experiments revealed that the morphological transformation of Pt thin films on untreated quartz substrates began through a void nucleation mechanism. As shown in Table 1, Batch 1 for Pt film on untreated substrate at 400 °C, the continuous Pt film exhibited the appearance of nanoscale voids randomly distributed across the surface. These initial voids indicate the onset of film instability, where atomic diffusion drives the breaking of film continuity to minimize surface and interface energies. At this stage, the film is not yet fully dewetted, but the nucleation of holes provides the driving force for subsequent morphological evolution.

Upon increasing the temperature to 500 °C, the density and size of voids markedly increased, and the film exhibited a more discontinuous structure. The coalescence of neighboring voids led to the thinning of interconnecting regions and the fragmentation of the Pt layer into irregular domains. This stage represents the advanced void nucleation and growth process, where enhanced surface diffusion accelerates mass transport away from the nucleated sites, leading to the destabilization of the film. At an annealing temperature of 600 °C, the morphological evolution of the Pt thin film became more pronounced compared to the lower-temperature stages. The void nucleation sites observed previously expanded significantly, leading to a wider spacing between the Pt regions. This widening of the gaps indicated the onset of film rupture and the gradual transition from a continuous thin film to a discontinuous structure.

At a thermal dewetting temperature of 700 °C, the Pt thin film underwent a significant morphological transformation, yet the complete formation of well-defined Pt nanodots was not observed. Instead, the micrograph reveals extensive rupture of the continuous Pt layer, where the voids previously initiated at lower temperatures expanded further, creating irregular channels and highly fragmented regions across the substrate. These enlarged voids resulted in the appearance of broad, tortuous gaps that isolated clusters of Pt but did not yet evolve into discrete, rounded nanoparticles.

For the Pt film (10 nm) on IPA-treated substrate at 400 °C, the morphology appears similar to that observed on the untreated substrate at the same temperature. The film exhibits nanoscale voids sparsely distributed across the surface, reflecting the initial stages of thermal dewetting. Compared with the untreated case, the IPA treatment does not result in a markedly different morphology at this early stage. The voids remain relatively small and isolated, and the film still retains semi-continuous coverage of the substrate.

At 500 °C, the Pt thin film on the untreated substrate exhibits irregular agglomeration,

Applied Science and Engineering Progress, Vol. 20, No. 1, 2027, 8253

Table 1: Comparative study on Pt film agglomeration on untreated and IPA-modified substrates.

Dewetting Temperature(°C)	Batch 1 : Pt film on an untreated substrate Thickness = 10 nm	Batch 2: Pt film on an IPA-treated substrate Thickness = 10 nm
400	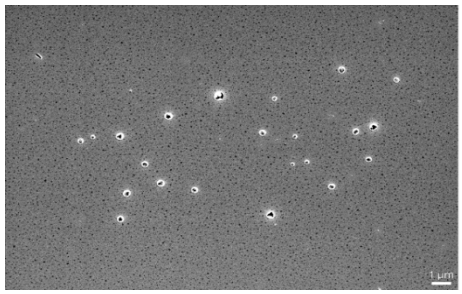	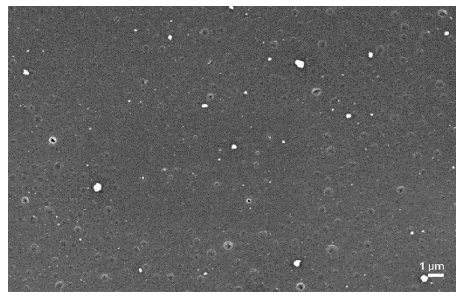
500	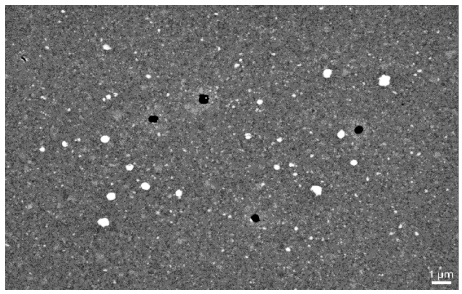	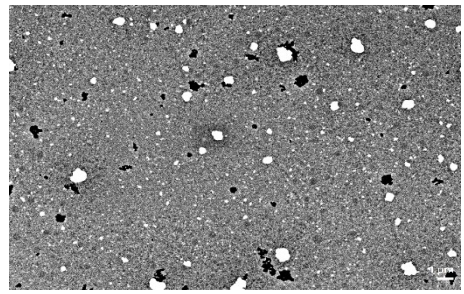
600	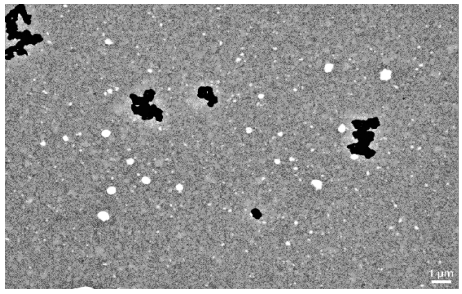	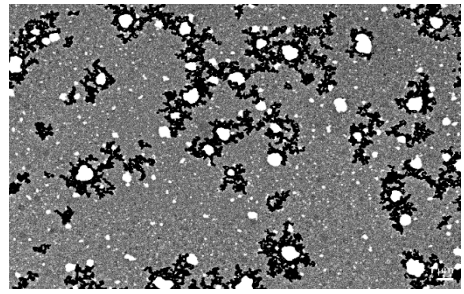
700	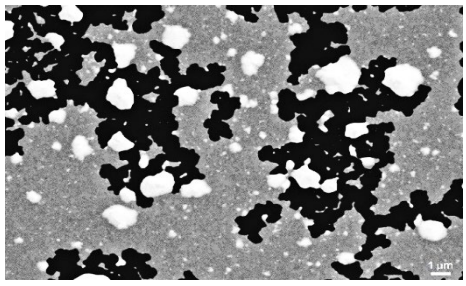	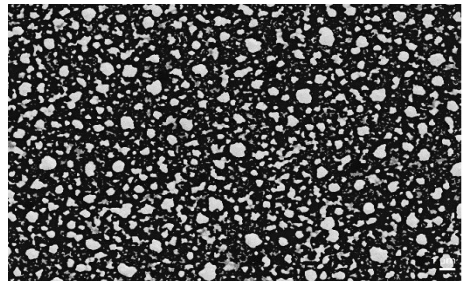

characterized by large, uneven clusters distributed across the surface with significant void formation. The particles appear coarsened and sparsely dispersed, indicating a less uniform dewetting process. In contrast, the Pt thin film on the IPA-treated substrate shows a finer and more homogeneous distribution of

nanoparticles. The metallic domains are smaller, more regularly shaped, and more evenly dispersed across the surface, with fewer large agglomerates. This clear morphological difference highlights the smoother and more controlled dewetting behavior achieved on the IPA-treated substrate compared with the untreated surface.

At 600 °C, the Pt film on the untreated substrate shows clear signs of agglomeration into large and irregular clusters. These clusters appear dark and bulky, with uneven shapes and sizes, and they are accompanied by a smaller number of fine particles scattered randomly on the surface. The overall surface looks rough and non-uniform, with a wide distribution of particle sizes. In contrast, the Pt film on the IPA-treated substrate breaks up into much smaller and more rounded nanoparticles. These particles are distributed more evenly across the substrate, creating a surface that appears finer, smoother, and more homogeneous compared to the untreated case. The difference in morphology between the two surfaces is clearly visible, with the untreated substrate dominated by large, irregular islands, while the IPA-treated substrate shows a dense layer of small and uniform particles.

At 700 °C, a clear visual difference is observed between platinum deposited on the untreated substrate and on the IPA-treated substrate. On the untreated surface, the platinum forms large, irregular agglomerates with rough edges, where many particles merge together and create non-uniform clusters scattered across the substrate. The size variation among the particles is wide, resulting in an overall uneven surface appearance. In contrast, the IPA-treated substrate exhibits much smaller and more rounded platinum nanoparticles that are distributed more evenly. The particles are well separated from one another, with less evidence of clustering or merging, giving the surface a finer and more uniform morphology. This contrast highlights how the untreated surface favors the growth of big, irregular clumps, while the IPA treatment promotes the formation of small, well-dispersed particles across the substrate.

3.2 *Absorbance spectra of Pt nanodots on untreated and IPA-treated substrates*

To evaluate the optical characteristics of the fabricated Pt nanodot arrays, ultraviolet–visible (UV–Vis) extinction spectra were measured using a BAS SEC2000 spectrometer in an absorbance-mode optical setup. Broadband illumination was provided by a tungsten–halogen light source (LS-1, Ocean Optics), covering the visible to near-infrared spectral region. During the measurement process, the incident light was first collimated and directed through the Pt nanodot array on the quartz substrate. The sample was mounted on a precision-controlled stage to ensure stable positioning and accurate optical alignment throughout the experiment. After passing through the sample, the absorbance light was collected by an optical fiber and transferred to the spectrometer for spectral acquisition. The absorbance spectra were recorded over a wavelength range of 400–850 nm in order to investigate the morphology-dependent optical response of the Pt nanodot structures.

The absorbance spectra indicate that Pt nanodots on the IPA-treated substrate deliver the superior optical response (Figure 4). The Pt nanodots on an IPA-treated sample (blue) show a sharper, more prominent band peaking near 600 nm with a maximum absorbance close to 0.35 a.u., consistent with smaller, more uniformly distributed nanodots that strengthen localized surface plasmon resonance (LSPR) and reduce off-resonant scattering. The narrower linewidth and higher peak-to-baseline contrast reflect improved spectral quality. In contrast, Pt nanodots on the untreated substrate (red) exhibit a broader, red-shifted feature about 560 nm with lower peak prominence, characteristic of larger, polydisperse aggregates and stronger inter-particle coupling that broaden the resonance and add radiative losses. Overall, the IPA surface treatment yields higher-quality and better-defined absorbance due to the smaller and more homogeneous nanodot morphology, whereas the untreated surface produces a weaker, broadened spectrum dominated by coarse clustering.

3.3 *Influence of isopropanol pretreatment on the morphological evolution of Pt nanodots during thermal dewetting*

As shown in Figure 5(a), at 400°C, the 10 nm platinum film on IPA-treated quartz remains mostly continuous but shows the first signs of breaking down, tiny holes (5-10 nm wide) begin forming at weak spots like grain boundaries and surface defects. At this temperature, platinum atoms have just enough energy to detach

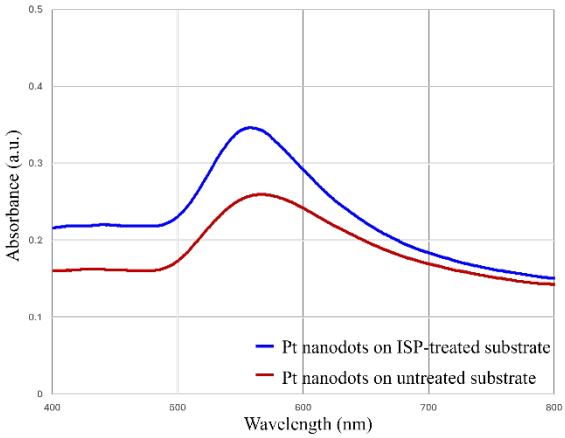

Figure 4 : Comparison of the absorbance spectra of Pt nanodot structures formed on untreated and IPA-treated quartz substrates after thermal dewetting.

from these defect sites but cannot move far across the surface, so the holes stay small, isolated, and do not merge together. This creates an incubation stage where the film is still intact but develops a uniform pattern of tiny nucleation points [42]. The IPA treatment helps by making the film stick better to the quartz, ensuring that when atoms do become mobile at higher temperatures, they spread evenly rather than clumping randomly. Essentially, 400°C sets up a controlled starter pattern of evenly-spaced weak points that will guide the formation of uniform nanoparticles when the temperature is increased further.

Figure 5(b) illustrates the behavior of Pt film at 500 °C. As the temperature increases continuously to 500°C, platinum atoms gain much more energy and mobility. The small holes from 400°C rapidly expand and merge together, causing the connected film to break apart into separate islands. On IPA-cleaned quartz, this dewetting process happens uniformly across the surface, creating evenly distributed platinum nanoislands with regular spacing. The islands show slightly angular shapes rather than perfect spheres, indicating the transformation is still in progress, but the overall pattern is very uniform due to the clean substrate surface.

As the temperature increased, these voids progressively expanded and interconnected Pt regions started to break apart into isolated islands through enhanced mass transport and agglomeration.

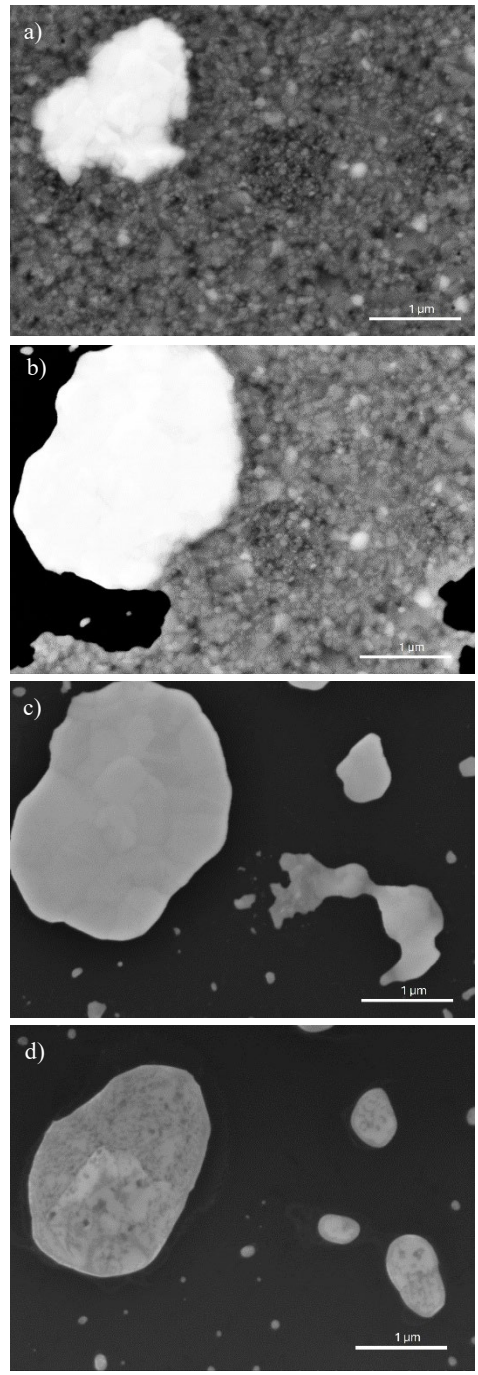

Figure 5: FE-SEM micrographs showing the morphological evolution of 10 nm Pt films deposited on IPA-treated quartz substrates after thermal annealing for 30 min at (a) 400 °C, (b) 500 °C, (c) 600 °C, and (d) 700 °C.

At the intermediate stage around 600 °C, as shown in Figure 5(c), the Pt structures exhibited irregularly shaped agglomerates with partially rounded boundaries, indicating active coalescence and surface diffusion. Upon further annealing at 700 °C, as shown in Figure 5(d), the Pt islands became more isolated and transformed into quasi-hemispherical nanodot-like structures and reduced interconnection between neighboring particles.

Figure 6 illustrates the AFM surface analysis of the Pt agglomeration on an untreated substrate, the AFM image reveals the formation of large and irregular Pt agglomerates with non-uniform height distribution across the scanned area. The corresponding line-profile analysis (X-X') shows substantial surface fluctuations, with peak heights reaching approximately 20 nm. The surface variation was distributed in the range of 10–16 nm, indicating severe particle coalescence and non-uniform mass redistribution during the thermal dewetting process.

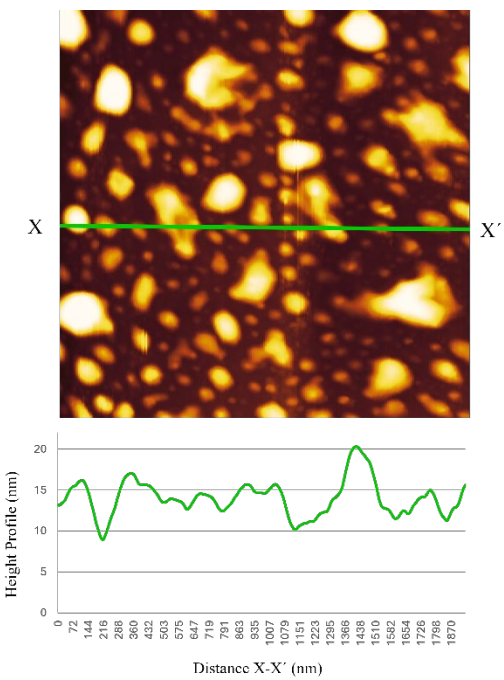

Figure 6: AFM analysis showing Pt agglomeration on the untreated substrate.

In contrast, the IPA-treated substrate exhibits a much more homogeneous distribution of Pt nanodots with significantly reduced particle size

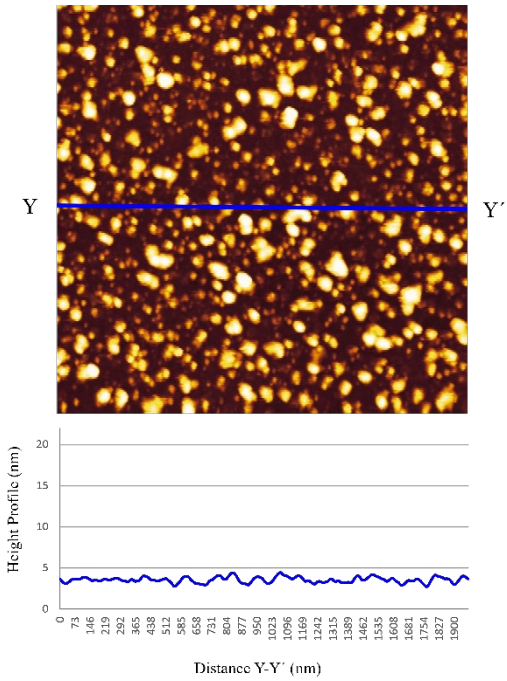

Figure 7: AFM analysis showing Pt agglomeration on the IPA-treated substrate.

and improved spatial separation, as shown in Figure 7. The corresponding AFM line-profile (Y-Y') demonstrates a considerably smoother surface morphology, with height fluctuations maintained within approximately 3–5 nm throughout the scanning distance.

Quantitatively, the IPA-treated substrate produced more uniformly distributed Pt nanodots with narrower height variation compared with the untreated substrate. These results clearly support the FE-SEM observations and confirm that IPA pretreatment promotes more controlled dewetting behavior, suppresses excessive Pt agglomeration, and enhances the uniformity of Pt nanodot formation.

3.4 *Surface coverage analysis of thermally dewetted Pt structures*

To provide a more reliable quantitative comparison, surface coverage analysis was performed using ImageJ software. The FE-SEM

Applied Science and Engineering Progress, Vol. 20, No. 1, 2027, 8253

images were converted into binary images through threshold processing, and the Pt-covered regions were quantitatively analyzed to determine the percentage of surface coverage. Based on the ImageJ analysis, the untreated substrate exhibited a relatively high Pt surface coverage of approximately 68.4%, as shown in Figure 8(a), indicating the presence of remaining interconnected Pt structures and incomplete film breakup after thermal dewetting. In contrast, as shown in Figure 8(b), the IPA-treated substrate showed a substantially lower Pt surface coverage of approximately 34.7%, confirming the formation of more isolated and discrete Pt nanodots with enhanced particle separation.

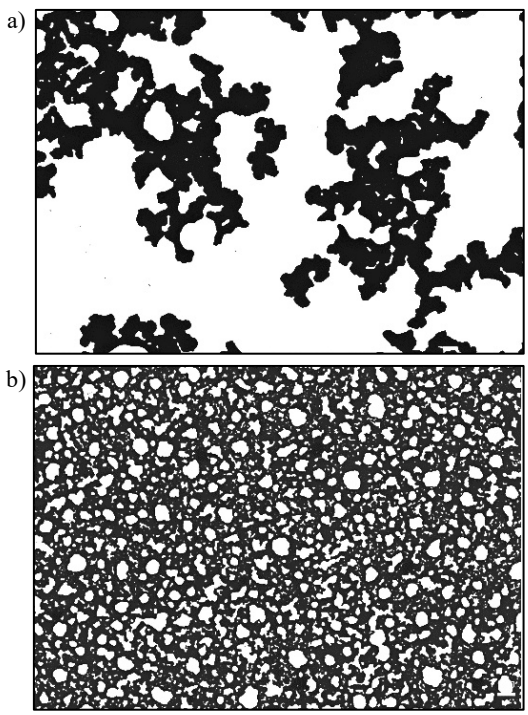

Figure 8: ImageJ-assisted quantitative surface coverage analysis of thermally dewetted 10 nm Pt films deposited on quartz substrates after annealing at 700 °C: (a) untreated substrate and (b) IPA-treated substrate.

The significant reduction in Pt surface coverage after IPA treatment suggests that the IPA-modified substrate promoted more effective thermal dewetting, enhanced film rupture, and suppressed excessive particle coalescence. These quantitative results support the FE-SEM observations and confirm that IPA surface treatment facilitated the transition from fragmented Pt film structures to uniformly dispersed Pt nanodot formation.

3.5 *Surface modification effects on thermal dewetting behavior and Pt nanodot formation*

Figure 9 illustrates the schematic diagram of the interfacial structure between a platinum (Pt) film and a glass substrate mediated by an intermediate IPA layer. At the bottom, the glass substrate contains surface silanol groups (Si–O–H), which are characteristic of hydroxylated silica surfaces. These silanol groups can form hydrogen bonds with the oxygen atom of the isopropanol (IPA) molecule. The IPA molecule is oriented such that its hydroxyl (–OH) group interacts with the silanol group, while its alkyl and branched carbon chains extend upward toward the Pt film [43]-[45].

At the top interface, the hydrogen atom of the IPA hydroxyl group interacts with the Pt surface, indicating possible weak adsorption or interfacial interaction between the metal film and the organic layer. The alkyl chain and branched structure provide a molecular bridge between the inorganic glass substrate and the metallic Pt film. Overall, the figure represents a molecular-level interfacial model explaining how IPA molecules can mediate adhesion or influence surface chemistry between a hydroxylated glass surface and a deposited platinum thin film. This increase in available polar functionalities raises the surface energy of the substrate (γ_S) [46]-[48]. According to Figure 10 and Young's equation (1), the balance of interfacial tensions at the three-phase contact line is given by

$$\gamma_I - \gamma_S = -\gamma_M cos\theta_c \qquad (1)$$

where

γ_M is the surface energy of the Pt (dot)

γ_S is the surface energy of the substrate

γ_I is the interfacial energy between the Pt (dot) and substrate

θ_c is the equilibrium contact angle of the Pt dot on the substrate

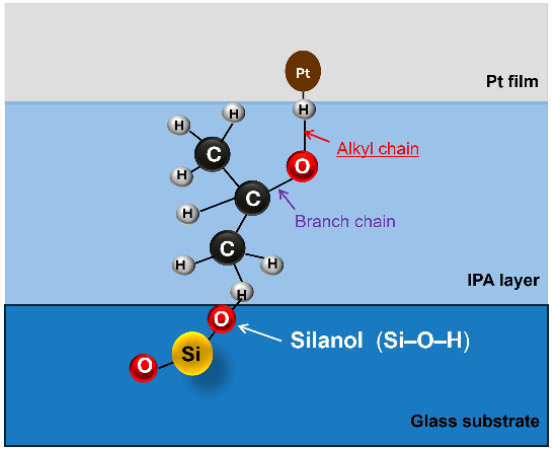

Figure 9: Proposed schematic illustration of molecular interactions at the Pt/IPA/quartz interface, including possible hydrogen bonding between IPA molecules and surface silanol groups.

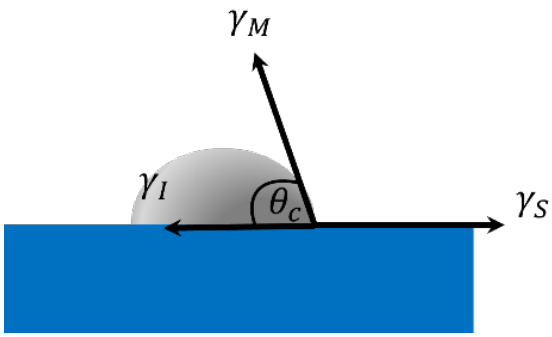

Figure 10: Schematic illustration of the equilibrium contact angle (θ_c) of a Pt nanodot on a quartz substrate according to Young's equation.

When the surface energy of the substrate increases via IPA treatment, equation (1) implies that $\cos\theta_c$ must increase (assuming γ_S and γ_I remain effectively constant), which in turn means that the equilibrium contact angle θ_c decreases. A lower contact angle reflects improved wettability of the Pt film on the quartz surface.

Improved wettability induced by IPA pretreatment significantly modifies the interfacial energy balance governing the thermal dewetting process, which can be described by Young's equation. The removal of adventitious hydrocarbons and the exposure of surface hydroxyl groups increase the solid–vapor interfacial energy (γ_s), leading to a reduction in the equilibrium contact angle (θ) and an enhancement of Pt–substrate adhesion. This increase in adhesion energy stabilizes the as-deposited Pt thin film, suppressing random pinhole formation and favoring the initiation of voids at energetically favorable and spatially reproducible defect sites, thereby establishing well-defined nucleation centers for subsequent dewetting.

During annealing, the presence of a homogeneous wetting layer results in a more uniform surface chemical potential landscape, enabling isotropic diffusion of Pt adatoms across the substrate rather than localized mass transport toward a limited number of dominant nuclei. Consequently, the dewetting process evolves in a controlled and spatially uniform manner, yielding Pt nanodot arrays with high areal density and narrow size distributions. In contrast, untreated substrates with lower γ_s and larger θ exhibit weaker adhesion and greater interfacial instability, leading to irregular film rupture, heterogeneous adatom diffusion, and the formation of fewer, highly polydisperse agglomerates. These results demonstrate that IPA pretreatment provides a simple yet effective route for tuning γ_s and the associated thermodynamic driving forces to achieve reproducible, high-density Pt nanodot arrays via thermal dewetting.

4 Conclusions

This study demonstrated that thermal dewetting of 10 nm Pt thin films on quartz substrates can produce self-assembled Pt nanodot structures without the use of lithographic processes. The experimental results revealed that annealing temperature and substrate surface condition strongly influenced the morphological evolution of Pt nanostructures during thermal dewetting. For untreated quartz substrates, the Pt films remained partially interconnected and formed irregular agglomerated structures even at high annealing temperatures. In contrast, IPA-treated substrates promoted more uniform film breakup and facilitated the formation of smaller, more isolated, and more uniformly distributed Pt nanodots. The in situ hot stage-assisted FE-SEM observations clearly confirmed the continuous morphological transformation of Pt films during annealing in the temperature range of 400–700 °C. Quantitative surface coverage analysis further supported the FE-

SEM observations, showing that IPA treatment enhanced the thermal dewetting process and reduced the remaining interconnected Pt structures on the substrate surface. In addition, the IPA-treated samples exhibited stronger and steeper absorbance features compared with untreated substrates, indicating morphology-dependent optical responses associated with improved Pt nanodot uniformity. Overall, the present study experimentally confirms that IPA surface treatment plays an important role in controlling the thermal dewetting behavior and nanodot formation of Pt thin films on quartz substrates.

Acknowledgments

This research was supported by University of Phayao and Thailand Science Research and Innovation Fund (Fundamental Fund 2026, Grant No. 2347/2568 and 2281/2568).

Author Contributions

N.S.: supervision, investigation, validation, formal analysis, review and editing. R.S.: methodology, formal design of experiments, investigation, data curation, visualization, and original draft preparation. P.P.: conceptualization, resources, data curation, writing and editing, funding acquisition, project administration, and correspondence. All authors have read and agreed to the published version of the manuscript.

Conflicts of Interest

The authors declare no conflict of interest.

Declaration of generative AI and AI-assisted technologies in the writing process

The authors utilized the ChatGPT tool to enhance the language and readability of the manuscript.

References

[1] N. H. Ramli, N. M. Nor, A. H. A. Bakar, N. D. Zakaria, Z. Lockman, and K. A. Razak, “Platinum-based nanoparticles: A review of synthesis methods, surface functionalization, and their applications,” *Microchemical Journal*, vol. 200, Art. no. 110280, May. 2024, doi: 10.1016/j.microc.2024.110280.

[2] S. Duan, Z. Du, H. Fan, and R. Wang. “Nanostructure Optimization of Platinum-Based Nanomaterials for Catalytic Applications,” *Nanomaterials*, vol. 8, no. 11, Art. no. 949, Nov. 2018, doi: 10.3390/nano8110949.

[3] A. Kumar, N. Das, and R. G. Rayavarapu. “Smart Platinum Nanostructures: A Journey from Synthesis to Advanced Theranostic Applications,” *Journal of Nanotheranostics*, vol. 4, no. 3, pp. 384–407, Aug. 2023, doi: 10.3390/jnt4030017.

[4] P. S.-Gallén, and K. Mužina, “Metallic nanoparticles at the forefront of research: Novel trends in catalysis and plasmonics,” *Nano Materials Science*, vol. 8, no. 3, pp. 534-555 May. 2026, doi: 10.1016/j.nanoms.2024.10.009.

[5] M. A. Darwish, W. A.-Elaziem, A. Elsheikh, and A. A. Zayed, “ Advancements in nanomaterials for nanosensors: a comprehensive review,” *Nanoscale Advances*, vol. 6, 4015, May. 2024, doi: 10.1039/d4na00214h.

[6] K. Yoshii, K. Yamaji, T. Tsuda, H. Matsumoto, T. Sato, R. Izumi, T. Torimoto, and S. Kuwabata, “Highly durable Pt nanoparticle-supported carbon catalysts for the oxygen reduction reaction tailored by using an ionic liquid thin layer,” *Journal of Materials Chemistry A*, vol. 4, no. 31, pp. 12152–12157, Jul. 2016, doi: 10.1039/c6ta04859e.

[7] R. Pothu et al., “High dispersion of platinum nanoparticles over functionalized zirconia for effective transformation of levulinic acid to alkyl levulinate biofuel additives in the vapor phase,” *Journal of Composites Science*, vol. 6, no. 10, Art. no. 300, Oct. 2022, doi: 10.3390/jcs6100300.

[8] E. Biehler, Q. Quach, and T.M. Abdel-Fattah, “Application of platinum nanoparticles decorating mesoporous carbon derived from sustainable source for hydrogen evolution reaction,” *Catalysts*, vol. 14, no. 423, Art. no. 423, Jul. 2024, doi: 10.3390/catal14070423.

[9] Y. Khan *et al.*, “Classification, synthetic, and characterization approaches to nanoparticles, and their applications in various fields of nanotechnology: a review, ” *Catalysts*, vol. 12,

no. 11, Art. no. 1386, Nov. 2022, doi: 10.3390/catal12111386.

[10] H. Park, D. J. Shin, and J. Yu, "Categorization of quantum dots, clusters, nanoclusters, and nanodots," *Journal of Chemical Education*, vol. 98, no. 3, pp. 703-709, Jan. 2021, doi: 10.1021/acs.jchemed.0c01403.

[11] T. Fujii et al*.,* "NMR evidence for energy gap opening in thiol-capped platinum nanoparticles," *Physical Review B*, vol. 105, no. 20, Art. no. 205403, May. 2022, doi: 10.1103/PhysRevB.105.L121401.

[12] D. Bera, Q. Lei, T. Teng-Kuan, and H. P. Holloway. 2010. "Quantum Dots and Their Multimodal Applications: A Review," *Materials*, vol. 3, no. 4, pp. 2260-2345, Mar. 2010, doi: 10.3390/ma3042260.

[13] S. Kunwar, M. Sui, P. Pandey, Z. Gu, S. Pandit, and J. Lee, "Improved configuration and LSPR response of platinum nanoparticles via enhanced solid state dewetting of In–Pt bilayers," *Scientific Reports*, vol. 9, Art. no. 1329, Feb. 2019, doi: 10.1038/s41598-018-37849-0.

[14] J. Jatschka, A. Dathe, A. Csáki, W. Fritzsche, and O. Stranik, "Propagating and localized surface plasmon resonance sensing-A critical comparison based on measurements and theory," *Sensing and Bio-Sensing Research*, vol. 7, pp. 62-70, Mar. 2016, doi: 10.1016/j.sbsr.2016.01.003.

[15] H. Park, A. K. L. Lim, A. P. Alivisatos, J. Park, and P. L. McEuen, "Fabrication of metallic electrodes with nanometer separation by electromigration," *Applied Physics Letters*, vol. 75, no. 2, pp. 301–303, Jul. 1999, doi: 10.1063/1.124354.

[16] S. M. Baig, and H. Abe, "Electrically interconnected platinum nanonetworks for flexible electronics," *ACS Omega*, vol. 10, no. 11, pp. 11562–11566, Mar. 2025, doi: 10.1021/acsomega.5c00237.

[17] S. Zhang *et al.,* "Gold–Platinum nanodots with high-peroxidase-like activity and photothermal conversion efficiency for antibacterial therapy," *ACS Applied Materials & Interfaces*, vol. 13, no.31, pp. 37535–37544, Jul. 2021, doi: 10.1021/acsami.1c10600.

[18] L. Sun *et al.,*"Silicon nanowires decorated with platinum nanoparticles were applied for photothermal-enhanced sonodynamic therapy," *Theranostics*, vol. 11, no. 19., pp. 9234-9242, Sep. 2021, doi: 10.7150/thno.58755.

[19] C. V. Thompson, "Solid-state dewetting of thin films," *Annual Review of Materials Research*, vol. 42, pp. 399–434, Aug. 2012, doi: 10.1146/annurev-matsci-070511-155048.

[20] J. Ye and C. V. Thompson, "Templated solid-state dewetting to controllably produce complex patterns," *Advanced Materials*, vol. 23, no. 14, pp. 1567–1571, Apr. 2011, doi: 10.1002/adma.201004095.

[21] P. Potejana, M. Yoshino, and M. Terano, "Efficient fabrication process of metal nanodot arrays using direct nanoimprinting method with a polymer mold," *International Journal of Automation Technology*, vol. 9, no. 6, pp. 629–635, Nov. 2015, doi: 10.20965/ijat.2015.p0629.

[22] P. Potejana, M. Yoshino, and M. Terano, "Fabrication of metallic nanodot arrays using nano-chemical stamping technique with a polymer stamp," *International Journal of Automation Technology*, vol. 10, no. 5, pp. 794–803, Sep. 2016, doi: 10.20965/ijat.2016.p0794.

[23] J. Nelayah *et al.,* "Mapping surface plasmons on a single metallic nanoparticle," *Nature Physics*, vol. 3, pp. 348–353, May 2007, doi: 10.1038/nphys575.

[24] P. Potejana, and N. Seemuang, "Fabrication of Metallic Nano Pillar Arrays on Substrate by Sputter Coating and Direct Imprinting Processes," *Applied Science and Engineering Progress*, vol. 14, no. 1, pp. 72-79, Jan. 2021, doi: 10.14416/j.asep.2019.09.001.

[25] A. Abduvalov**,** M. Kaikanov, and A. Tikhonov, "Solid-State Dewetting of Thin Silver Films into Spherical Nanoparticles under High-Current Pulsed Ion Beam Irradiation," *ACS*, vol. 8, no. 35, pp. 31954–31961, Aug. 2023, doi: 10.1021/acsomega.3c03743.

[26] W. Ratanathavorn, N. Boohuad, and R. Rungruang, "Enhanced Broad-Spectrum Protection Against High-Energy Visible Light Using Co-Doped Ag_2O and $ZnO–TiO_2$ Nanocomposites," *Applied Science and Engineering Progress*, vol. 19, no. 2, pp. 72-79 Art. no. 7909, Apr. 2026, doi: 10.14416/j.asep.2025.09.009.

[27] M. Stepanova, S. K. Dew, and I. P. Soshnikov, "Copper nanopattern on SiO_2 from sputter etching a Cu/SiO_2 interface," Apply Physics

Letters, vol. 86, 073112, Feb. 2005, doi: 10.1063/1.1864247.

[28] S. Jahangir, X. Cheng, H. H. Huang, J. Ihlefeld, and V. Nagarajan, "In-situ investigation of thermal instabilities and solid state dewetting in polycrystalline platinum thin films via confocal laser microscopy," *Journal of Applied Physics*, vol. 116, Art. no. 163511, Oct. 2014, doi: 10.1063/1.4898691.

[29] Y. Lee, K. Koh, H. Na, K. Kim, J.-J. Kang, and J. Kim, "Lithography-Free Fabrication of Large Area Subwavelength antireflection structures using thermally dewetted Pt/Pd alloy etch mask," *Nanoscale Research Letters*, vol. 4, no. 364, Jan. 2009, doi: 10.1007/s11671-009-9255-4.

[30] J.A. Badán et al., "Silver nanoparticle arrays onto glass substrates obtained by solid-state thermal dewetting: a morphological, structural and surface chemical study," *Nanomaterials*, vol. 12, Art. no. 617, Feb. 2022, doi: 10.3390/nano 12040617.

[31] S. N. Bonvicini, and Y. Shi, "Formation and Removal of Alloyed Bimetallic Au–Ag Nanoparticles from Silicon Substrates for Tunable Surface Plasmon Resonance," *ACS Applied Nano Materials*, vol. 5, no. 10, pp. 14850–14861, Sep. 2022, doi: 10.1021/acsanm. 2c03154

[32] B. Medasani, Y. H. Park, and I. Vasiliev, "Theoretical study of the surface energy, stress, and lattice contraction of silver nanoparticles," *Physical Review B*, vol. 75, Art. no. 235436, Jun. 2007, doi:10.1103/PhysRevB.75.235436.

[33] F. Bignolia et al., "Effect of annealing on mechanical properties and thermalstability of ZrCu/O nanocomposite amorphous films synthetized by pulsed laser deposition," *Materials&Design*, vol. 22, Art. no. 110972, Jul. 2022, doi: 10.1016/j.matdes.2022.110972.

[34] N. N. Mahmoud et al., "The effect of surface-modified gold nanorods on the early stage of embryonic development and angiogenesis: insight into the molecular pathways," *International Journal of Molecular Sciences*. vol. 22, no. 20, Art. no. 11036, Oct. 2021, doi: 10.3390/ijms222011036.

[35] R. Abbas *et al.,* "Silver Nanoparticles: Synthesis, Structure, Properties and Applications," *Nanomaterials*, vol. 14, no. 17, Art. no. 1425, Aug. 2024, doi: 10.3390/nano14171425.

[36] D. Sonawane, A. Choudhury, and P. Kumar, "New insights into dewetting of Cu thin films deposited on Si," *Langmuir*, vol. 36, no. 20, pp. 5534–5545, Apr. 2020, doi: 10.1021/acs. langmuir.0c00575.

[37] R. Brown, B. Lönn, R. Pfeiffer, H. Frederiksen, and B. Wickman, "Plasma-induced heating effects on platinum nanoparticle size during sputter deposition synthesis in polymer and ionic liquid substrates," *Langmuir*, vol.37, no. 29, pp. 8821–8828, Jul. 2021, doi : 10.1021/acs. langmuir.1c01190.

[38] J. Liu, J. Wang, M. Li, and H. Zhang, "High quality Pt–Pt metal bonding for high temperature packaging," *Micromachines*, vol. 13, no.9, Art. no. 1543, Sep. 2022, doi: 10.3390/mi13091543.

[39] N. Ramanamane, and M. Pita, "Surface-Tuned Quartz Particles for Oil–Water Separation: SEM Characterization, Coating Effects, and Predictive Modelling," *Surfaces,* vol. 8, Art. no. 67, Aug. 2025, doi: 10.3390/surfaces8030067.

[40] H. Kim, J. Hong, C. Kim, E.-Y. Shin, M. Lee, Y.-Y. Noh, B. Park, and I. Hwang, "Impact of Hydroxyl Groups Boosting Heterogeneous Nucleation on Perovskite Grains and Photovoltaic Performances," *The Journal of Physical Chemistry C*, vol. 122, no. 29, pp. 16630-16638, Jul. 2018, doi: 10.1021/acs.jpcc. 8b05374.

[41] J.-M. Lee, and B.-I. Kim, "Thermal dewetting of Pt thin film: etch-masks for the fabrication of semiconductor nanostructures," *Materials Science and Engineering: A*, vol. 449–451, pp. 769-773, Mar. 2007, doi: 10.1016/j.msea.2006. 02.403.

[42] J. Ye, "Fabrication of ordered arrays of micro- and nanoscale features with control over their shape and size via templated solid-state dewetting," *Scientific Reports*, vol. 5, Art. no. 9823, May 2015, doi: 10.1038/srep09823.

[43] Y. Naruke, S. Kosaka, T. Nakano, G. Kikugawa, and T. Ohara, "A molecular dynamics study on mass transport characteristics in the vicinity of SiO_2–water/IPA interfaces," *International Journal of Heat and Mass Transfer*, vol. 84, pp. 584-591, May 2015, doi: 10.1016/j.ijheatmas stransfer.2015.01.051.

[44] L. T. Zhuravlev, and V. V. Potapov, "Density of silanol groups on the surface of silica precipitated from a hydrothermal solution,"

Physical Chemistry of Surface Phenomena, vol. 80, pp. 1119–1128, Jul 2006, doi: 10.1134/S00 36024406070211.

[45] S. Chibani, C. Michel, F. Delbecq, C. Pinel, and M. Besson, "On the key role of hydroxyl groups in platinum-catalysed alcohol oxidation in aqueous medium," *Catalysis Science & Technology*, vol. 3, pp. 339-350, Aug. 2013, doi: 10.1039/c2cy20363d.

[46] M. J. Ungerer, D. S. Carballal, A. C. Essadek, C. G. C. E. v. Sittert, and N. H. d. Leeuw, "Interaction of H_2O with the platinum Pt (001), (011), and (111) surfaces: a density functional theory study with long-range dispersion corrections," *The Journal of Physical Chemistry C*, vol. 123, no. 45, pp. 27465-27476, Sep. 2019, doi: 10.1021/acs.jpcc.9b06136.

[47] D. Wu, X. Guo, H. Sun, and A. Navrotsky, "Energy landscape of water and ethanol on silica surfaces," *Journal of Physical Chemistry*, vol. 119, no. 27, pp.15428-15433, Jun. 2015, doi: 10.1021/acs.jpcc.5b04271.

[48] B. Majhy, P. Priyadarshinia, and A. K. Sen, "Effect of surface energy and roughness on cell adhesion and growth-facile surface modification for enhanced cell culture," *RSC Advances*, vol. 11, pp. 15467-15476, Apr. 2021, doi: 10.1039/ d1ra02402g.